

Analysis of the flow behavior of concentrated polymer solutions through transient network models. Part I, simple shear

J. Zaragoza and O. Manero

*Departamento de Polímeros, Instituto de Investigaciones en Materiales,
Universidad Nacional Autónoma de México, Apdo. Postal 70-360,
04510 México, D.F.*

(recibido el 20 de mayo de 1986; aceptado el 6 de enero de 1987)

Abstract. Transient Network Models are used to simulate the rheological behavior of concentrated solutions of polymeric materials. A fairly good agreement with the experimental situation is obtained if a conformation dependent non-affine motion of the segments forming the polymeric network is considered. The introduction of non-affinity into the diffusion equation for the configurational probability function in these models gives rise to the prediction of important macroscopic transport properties. For example, the prediction of a finite second normal-stress difference and a limited small deformation of the network segments in simple shear, together with distinctive features in transient flows.

Resumen. En este trabajo, el comportamiento reológico de soluciones concentradas poliméricas es analizado con base en las predicciones de los modelos de redes transitorias. La consideración de un movimiento no afín de los segmentos que forman la red polimérica es factor indispensable para una adecuada predicción de los resultados experimentales. A partir de los momentos de la función de distribución configuracional de los segmentos, es posible predecir importantes propiedades de transporte. Por ejemplo, la predicción de la segunda diferencia de esfuerzos normales de la solución junto con una limitada deformación de los segmentos en flujo cortante simple, y la predicción de propiedades interesantes en flujos transitorios.

PACS: 81.20sh; 47.50+d; 66.20+d; 61.25 Hq

1. Introduction

It is understood that polymeric fluids are viscous fluids which contain an elastic substructure or network of entangled macromolecular chains. Configurational changes in the microstructure of these systems produced by flow are the cause of the observed macroscopic behavior of flowing polymeric liquids. To model this behavior, transient network theories have been proposed. Originally developed by Green and Tobolsky [1], Lodge [2] and Yamamoto [3], they fundamentally envisage a concentrated polymer solution composed of elastic segments or strands joined through temporary junctions constantly undergoing creation and destruction processes. In Yamamoto's theory, a segment is represented by an end-to-end vector joining two entanglement points. The distribution function for the segments follows the equation

$$\frac{\delta\psi}{\delta t} + \nabla \cdot \dot{\mathbf{r}}\psi = G - \beta\psi, \quad (1)$$

where $\dot{\mathbf{r}}$ is the rate of change of the end-to-end vector \mathbf{r} , G is the rate of creation and β is the rate of destruction of the network junctions. Given a macroscopic motion

$$\dot{\mathbf{r}} = \mathbf{\Gamma} \cdot \mathbf{r}, \quad (2)$$

where $\mathbf{\Gamma}$ is the velocity gradient tensor, Eq. (1) can be solved for various flow situations and the macroscopic rheological functions are evaluated by calculating the moments of the distribution function. The creation function of segments G is generally assumed Gaussian for the initial distribution of the end-to-end distance of the segments. This assumption is based on the fact that the segments are created at constant rate and they have at the instant of creation, the same distribution of free chains. The form of the rate of destruction function β gives rise to a variety of predictions from the model. It is generally assumed by most authors, that β may depend on the mean squared extension of the segments $\langle r^2 \rangle^{1/2}$. This idea relates the destruction rate to the elastic content of the system. In fact, Helmholtz free energy for transient network systems is given in terms of the excess

free energy and it is a measure of the deformation of the network with respect to its equilibrium value. If the destruction function is related to the end-to-end distance between entanglements, then this function is necessary dependent on the entangled state of the network.

To further complement the model, Phan-Thien and Tanner [4] and Johnson and Segalman [5] introduced the idea of "non-affine" motion to account for differences in the deformation between the network and the imposed flow. In this case, an "effective" velocity gradient tensor is defined:

$$\mathbf{L} = \mathbf{\Gamma} - \epsilon \mathbf{D}, \quad (3)$$

where D is the rate of deformation tensor ($\mathbf{D} = (1/2)(\mathbf{\Gamma} + \mathbf{\Gamma}^T)$) and ϵ is a constant termed slip parameter.

2. The stress in the network

The stress in a network is obtained by determining the forces related to the changes in free energy of the system undergoing a virtual deformation. In a Gaussian network under isothermal conditions, the decrease in the Helmholtz free energy of the system is equal to the work performed by the system on the surroundings [6]:

$$-dA = \mathbf{F} \cdot d\mathbf{r}, \quad (4)$$

where

$$A = -KT \ln C \quad (5)$$

and

$$C = L \left(\frac{3}{2} N \right)^{3/2} e^{-3Nr^2/2}. \quad (6)$$

N is the number of statistical sub-units making up the chain between entanglement points, L is a constant, T the temperature and \mathbf{F} the force. If we assume C is Gaussian (Eq. 16), this leads to a linear force in the segments given by

$$\mathbf{F} = -3NkT \mathbf{r}; \quad (7)$$

and in this case the stress tensor is expressed as

$$\mathbf{r} = \langle \mathbf{F}\mathbf{r} \rangle = -3NkT\langle \mathbf{r}\mathbf{r} \rangle, \quad (8)$$

where the brackets mean the statistical average integrated over the configurational space.

If C is non-Gaussian, this is

$$-\ln C = \frac{3}{2}Nr^2\{1 + a_2r^2 + \dots\}, \quad (9)$$

where a_2 is a constant, the relationship Eq. (8) no longer holds. In this case, up to first order, the force is given by

$$\mathbf{F} = -3NkT(1 + 2a_2\langle r^2 \rangle)\mathbf{r} \quad (10)$$

and the stress tensor by

$$\mathbf{r} = \langle \mathbf{F}\mathbf{r} \rangle = -3NkT(1 + 2a_2\langle r^2 \rangle)\langle \mathbf{r}\mathbf{r} \rangle. \quad (11)$$

In obtaining Eq. (11), Peterlin's preaveraged approximation has been used [7]. In this, the function at each instant is replaced by its value at the mean square end-to-end distance $\langle r^2 \rangle^{1/2}$ which exists at that moment. Equation (10) assumes that the nonlinearity of the force can be treated in a mean field fashion (in the spirit of the preaveraging approximation for the Oseen interaction tensor [8]). This approximation for the force is reasonable as long as the nonlinearities can be considered as small perturbation. It clearly breaks down when the applied force becomes strong.

Further departures from Gaussian statistics can be obtained by considering more terms in the expansion Eq. (9). By extending the series to higher order, the expression for the stress tensor may be given by

$$\mathbf{r} = \left(\frac{\beta_0}{1 - \langle r^2 \rangle} \right) \langle \mathbf{r}\mathbf{r} \rangle, \quad (12)$$

where β_0 is constant.

3. The rate of destruction function

As it was mentioned, β is related to the elastic content of the system and depends on the degree of deformation of the network. Therefore, it is proportional to the excess free energy and to the existing force in the segments. The assumption that β is constant, implies that the entanglement density of the network does not change with the imposed flow, giving rise to a constant viscosity behavior and constant normal stress coefficients in shear flow. This case corresponds to a linear force between entanglements (Eq. (7)) equivalent to Hookean springs. Predictions show agreement with results in the linear viscoelastic range.

The first order departure from Gaussian statistics implies that β must be conformation-dependent. In agreement with the expression for the force (Eq. (10)), in this case β is given by

$$\beta = \beta_0 \{1 + \sigma \langle r^2 \rangle\}, \quad (13)$$

where β_0 and σ are constants. This expression for the rate of destruction function has been discussed by Fuller and Leal [9] in their quadratic destruction model. This model still uses linear springs in the segments by restricting the range of values given to σ allowing the use of Eq. (8) for the stress. Predictions of this model in simple shear show nonlinear behavior, such as a decrease in entanglement densities with increasing rate of shear, consequently giving rise to a shear-thinning viscosity and variable normal-stress coefficients.

Murayama [10] analyzed the macroscopic effects of the second order departure from Gaussian statistics by adding the quadratic term in the series expansion with variable coefficients. The force may increase at first proportional to $\langle r^2 \rangle$, but at large deformations it increases up to infinity because of the limited extensibility of the network segments. Indeed, Phan-Thien and Tanner [4] assumed that the chain-dissociation coefficient is a function of the mean square average of the end-to-end distance of the network segments and increases exponentially with increasing strain. This assumption is closely related with the spring force implied in the expression for

the stress Eq. (12) and accordingly, the destruction function may be given by

$$\beta = \frac{\beta_0}{1 - \langle r^2 \rangle}. \quad (14)$$

4. Non-affine Motion

Differences in deformation between the network and the imposed flow give rise to what is called “slip mechanism” or non-affine motion. By introducing an effective velocity gradient tensor Eq. (3), additional nonlinear characteristics are given to the model. For example, in a mean-field approximation, non-affine motion is the cause of macroscopic effect such as the second normal-stress difference in shear flow with variable coefficients. As a first approximation, the slip parameter ϵ might be thought to be a constant. However, in the non-Gaussian regime of nonlinear spring forces acting on the segments, the relationship between the deformation of the network and the linear relation of Eq. (2) of the imposed flow is not simple. In fact, the motion of the network with respect to the imposed flow depends strongly on the hydrodynamic interaction and the non-free draining character of the segments forming the polymeric network. Accordingly, we can analyze this dependency by distinguishing two different flow regimes: the intermediate force regime and the strong force regime. As it has been pointed out by Rabin and Dash [8], in the intermediate force regime the hydrodynamic interaction tends to increase with increasing force and the non-free draining character of the segments is enhanced, as predicted by Peterlin in shear and elongational flows [11]. This produces coupled forces among the segments, affecting the motion of the whole network with respect to the imposed flow and given rise to the slip mechanism. However, in the strong force regime, the external force penetrates most of the length scales in the segments and the hydrodynamics interaction decreases. In Rabin and Dash analysis the Rouse case (free draining case or negligible hydrodynamic interaction) is approached asymptotically with increasing force. This effectively reduces the non-affine motion,

suggesting that the segments are gradually being aligned in the flow direction reducing their hydrodynamic interaction that prevents the slip mechanism. To model this behavior, the following expression for the non-affine motion is proposed:

$$\epsilon = \epsilon \langle r^2 \rangle = \frac{\epsilon_0}{N \langle r^2 \rangle + 3}, \quad (15)$$

where ϵ_0 is of order unity. In this equation, the slip mechanism is reduced with increasing deformation of the segments end-to-end distance. It also implies that the segments are deformed from a coiled configuration corresponding to free chains into an ellipsoidal-like shape due to the imposed flow [12]. Consequently, by Eq. (15), non-affine motion is confined to an initial degree of deformation and initial transients in unsteady flow.

The following results in simple shear flow analyze the macroscopic effects of a conformation-dependent slip coefficient. Of course, the validity of the model will depend upon agreement with available experimental data.

5. Results

The macroscopic rheological functions are obtained from the moments of the distribution function. The expression for the momenta in simple shear are worked out by multiplying Eq. (1) by $\mathbf{r}\mathbf{r}$ and averaging the resulting equation in the configurational space. In simple shear, for the velocity gradient tensor given by $\mathbf{\Gamma} = \frac{\dot{\gamma}}{2} \begin{bmatrix} 0 & 1 & 0 \\ 0 & 0 & 0 \\ 0 & 0 & 0 \end{bmatrix}$ we

have

$$\begin{aligned}
 \frac{d}{dt}\langle x^2 \rangle + \left\{ h - \alpha \left(1 - \epsilon(\langle r^2 \rangle) \right) \right\} \langle x^2 \rangle &= \alpha \langle xy \rangle + \frac{L}{3N\beta_0} \\
 \frac{d}{dt}\langle y^2 \rangle + \left\{ h + \alpha \left(1 - \epsilon(\langle r^2 \rangle) \right) \right\} \langle y^2 \rangle &= -\alpha \langle xy \rangle + \frac{L}{3N\beta_0} \\
 \frac{d}{dt}\langle xy \rangle + h \langle xy \rangle &= \frac{\alpha}{2} \langle y^2 \rangle - \frac{\alpha}{2} \langle x^2 \rangle \\
 \frac{d}{dt}\langle z^2 \rangle + h \langle z^2 \rangle &= \frac{L}{3N\beta_0}
 \end{aligned} \tag{16}$$

where

$$h = \frac{\beta}{\beta_0} = \frac{1}{1 - \langle r^2 \rangle} \quad \text{rmand} \quad \alpha = \frac{\dot{\gamma}}{\beta_0}.$$

Another quantity of interest is the birefringence, defined as

$$\Delta n = B \left\{ \langle x^2 - y^2 \rangle^2 + 4 \langle xy \rangle^2 \right\}^{1/2}. \tag{17}$$

Birefringence is a measure of the degree of anisotropy of the flowing solution. When is measured in a flowing system, it provides insight into the actual degree of deformation of the network. In Eq. (16) we are considering the Warner expression for the force and the destruction function β , corresponding to the non-Gaussian regime.

In simple shear, the rheological functions are

$$\frac{S}{KT} = \frac{L}{\beta_0} \cdot \frac{\alpha \left\{ 1 - \epsilon(\langle r^2 \rangle) \right\}}{h^2 - 4\alpha^2}, \tag{18}$$

$$\frac{N_1}{KT} = \frac{L}{\beta_0} \cdot \frac{2\alpha^2 \left\{ 1 - \epsilon(\langle r^2 \rangle) \right\}}{h^2 - 4\alpha^2} \tag{19}$$

and

$$\frac{N_2}{KT} = -\frac{N_1}{2} \epsilon(\langle r^2 \rangle), \tag{20}$$

where S , N_1 and N_2 are the shear-stress and first and second normal-stress differences.

6. Steady simple shear

At relatively high values of the shear rate, a major decrease in junction concentration only is possible when $\epsilon = 0$. Non-affine motion in simple shear produces a small degree of deformation of the segments, effectively preventing the breakage of the junctions. In Fig. 1, a constant slip parameter is used to show this. The normalized birefringence is plotted with the velocity gradient for $\epsilon = 0.2$, becoming asymptotic over a range of shear rates, effectively approaching a small value at high velocity gradients. Consequently, we have on this asymptote

$$\Delta n \sim \langle r^2 \rangle \sim O\left(\frac{1}{N}\right),$$

and from Eq. (12)

$$\tau \doteq \beta_0 \langle \mathbf{r}\mathbf{r} \rangle.$$

This expression is similar to Eq. (8) to order $(1/N)$ for linear springs. Therefore, by setting ϵ to a constant value, it gives results similar to those obtained from the quadratic destruction model.

On the other hand, for $\epsilon = 0$, a major deformation can be expected at high shear rates, and the correct expression for the stress in this case is given in Eq. (12), corresponding to non-linear spring in the non-Gaussian regime of deformations. In Fig. (2), a conformation-dependent slip parameter Eq. (15) is used, producing a shear-thinning viscosity. Similar results are obtained for the first and second normal stress coefficients, in agreement with available experimental results for concentrated polymer solutions.

7. Unsteady simple shear

Solution to the coupled differential equations (16) was obtained by using a 4th. order Runge-Kutta routine. Results are given in

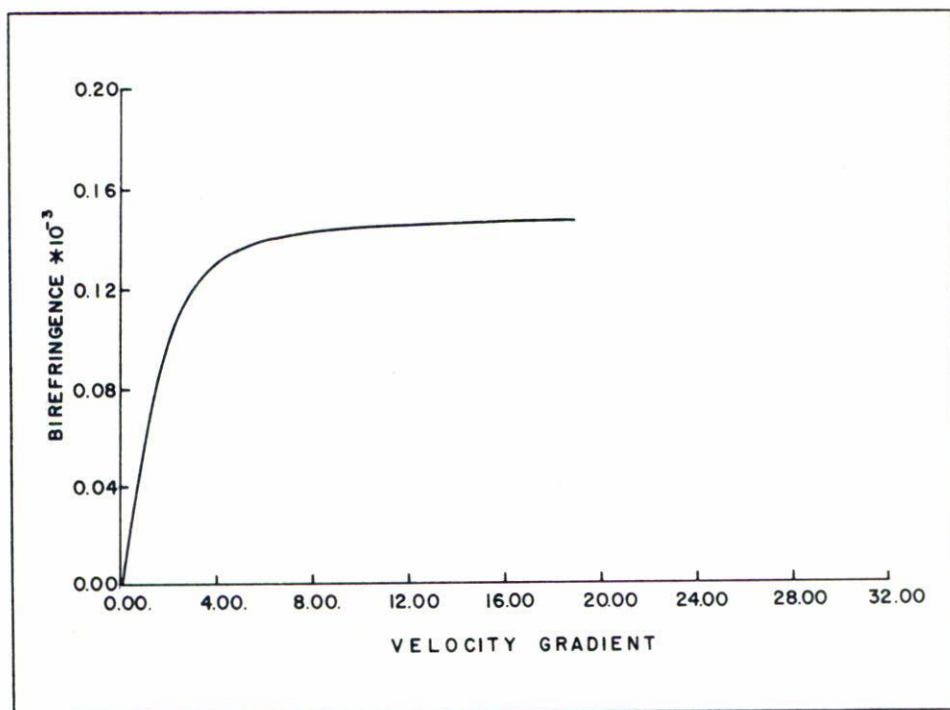


FIGURE 1. Normalized birefringence vs. velocity gradient in simple shear flow, for constant slip coefficient ($\epsilon = 0.2$).

Figs. 3–7, showing the response of the shear stress and normal stress differences to a start-up flow in simple shear. Three different cases were considered: $\epsilon = 0$, $\epsilon = 0.1$ and $\epsilon_0 = 0.5$ in Eq. (15). Figs. 3–5 show the shear-stress grow function S/α depicting a steady-state level which decreases with increasing rate of shear (shear-thinning). With affine motion, a monotonic increase is observed for all values of α considered. A constant slip parameter gives different results: overshoots are shown with damped oscillations at high shear rates. The inclusion of a conformation-dependent slip parameter shows the same features as the previous case, but the oscillations are quickly damped out. This latter case is in better agreement with experimental data. Finally, Figs. 6 and 7 show results for the normal stress

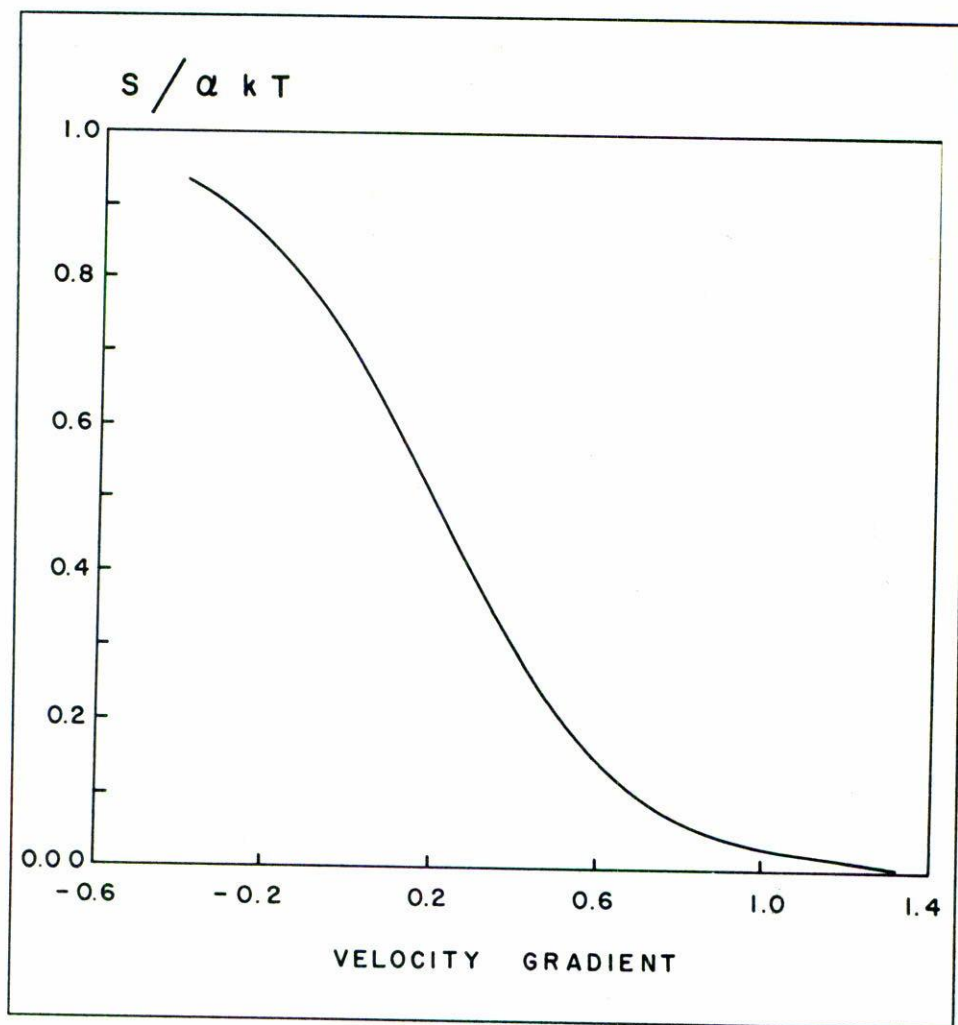


FIGURE 2. Shear viscosity vs. velocity gradient with conformation dependent slip parameter.

differences, depicting a similar qualitative behavior exhibited by the stress, also in agreement with the experiments made on a flowing polymeric solution of high concentration.

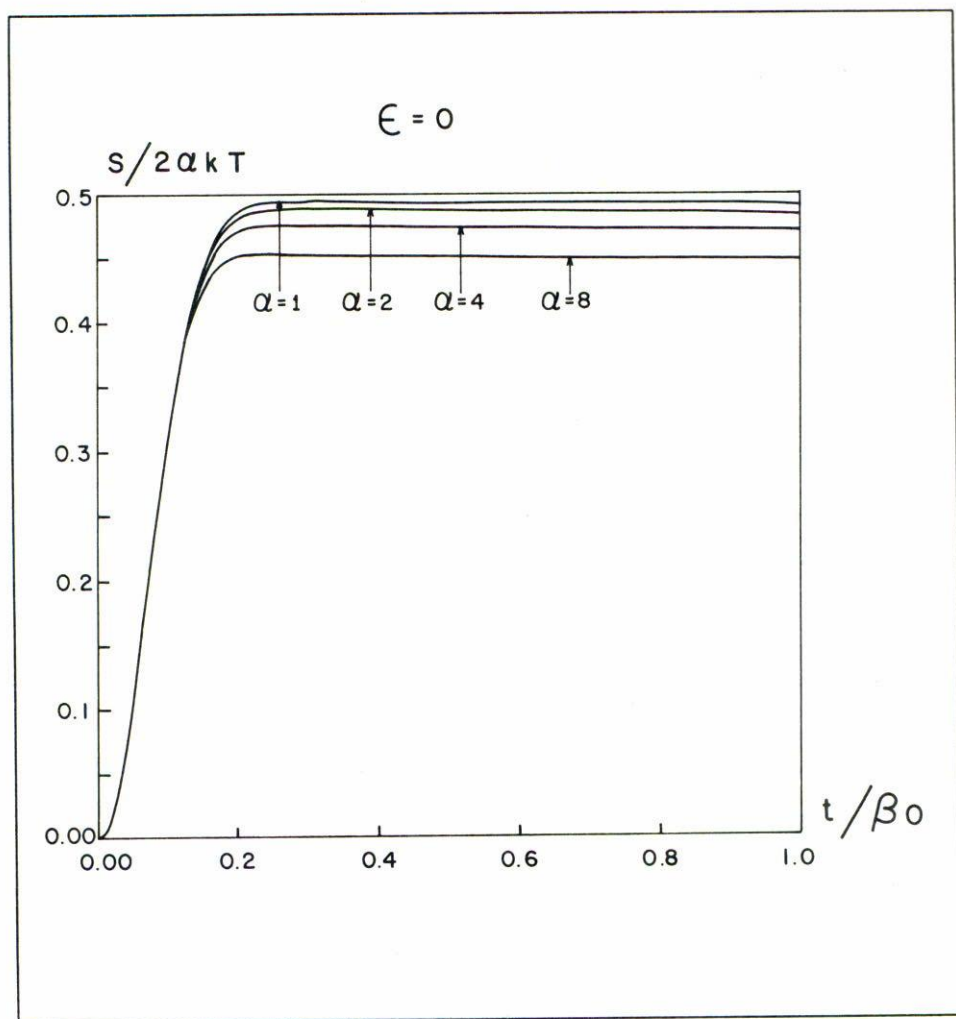


FIGURE 3. Stress growth function vs. non-dimensional time for various values of the velocity gradient. Affine motion ($\epsilon = 0$).

It is important to observe that the inclusion of non-affine motion gives rise to the prediction of a second normal stress coefficient (see Eq. (20)). In simple shear, concentrated polymeric solutions or melts

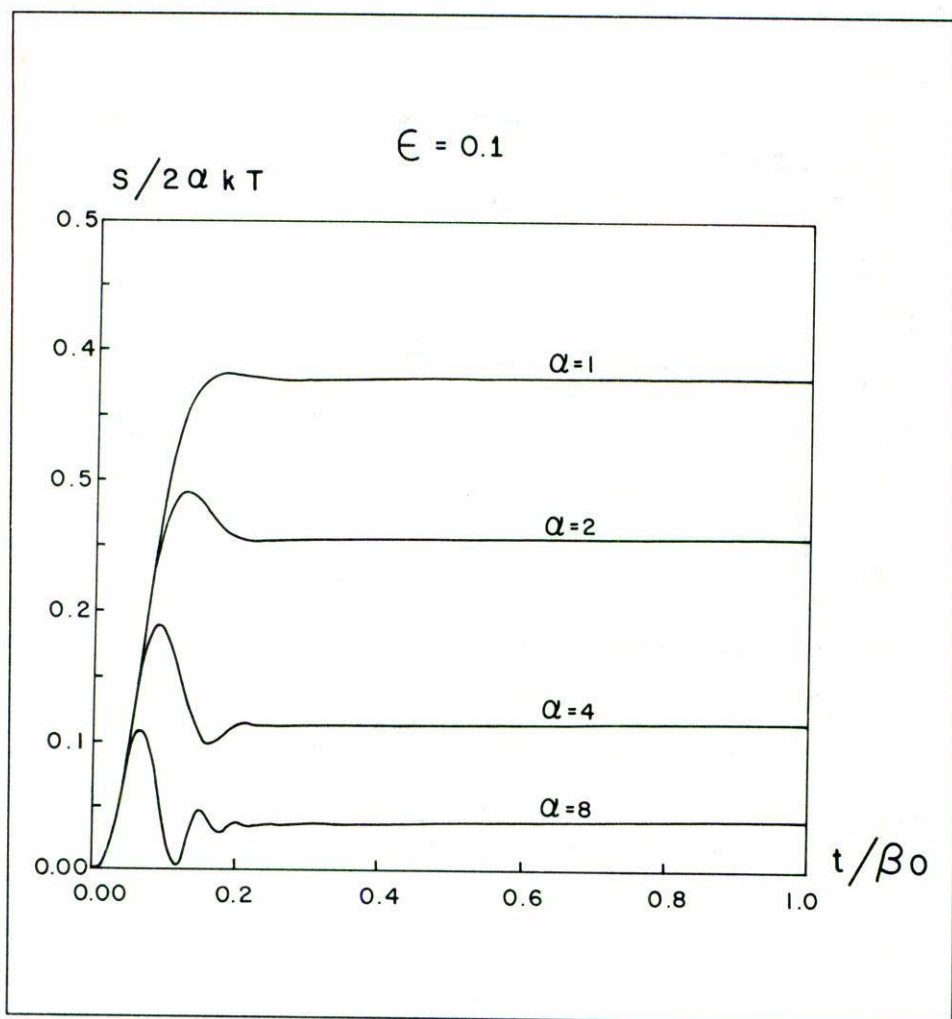


FIGURE 4. Same as in Fig. 3, with constant slip parameter ($\epsilon = 0.1$).

show a finite value of this coefficient which is much lower than the first normal stress coefficient and has opposite sign. Experimental data for the second normal stress difference is very scarce, although there is some evidence that N_2 is about $-0.1N_1$.

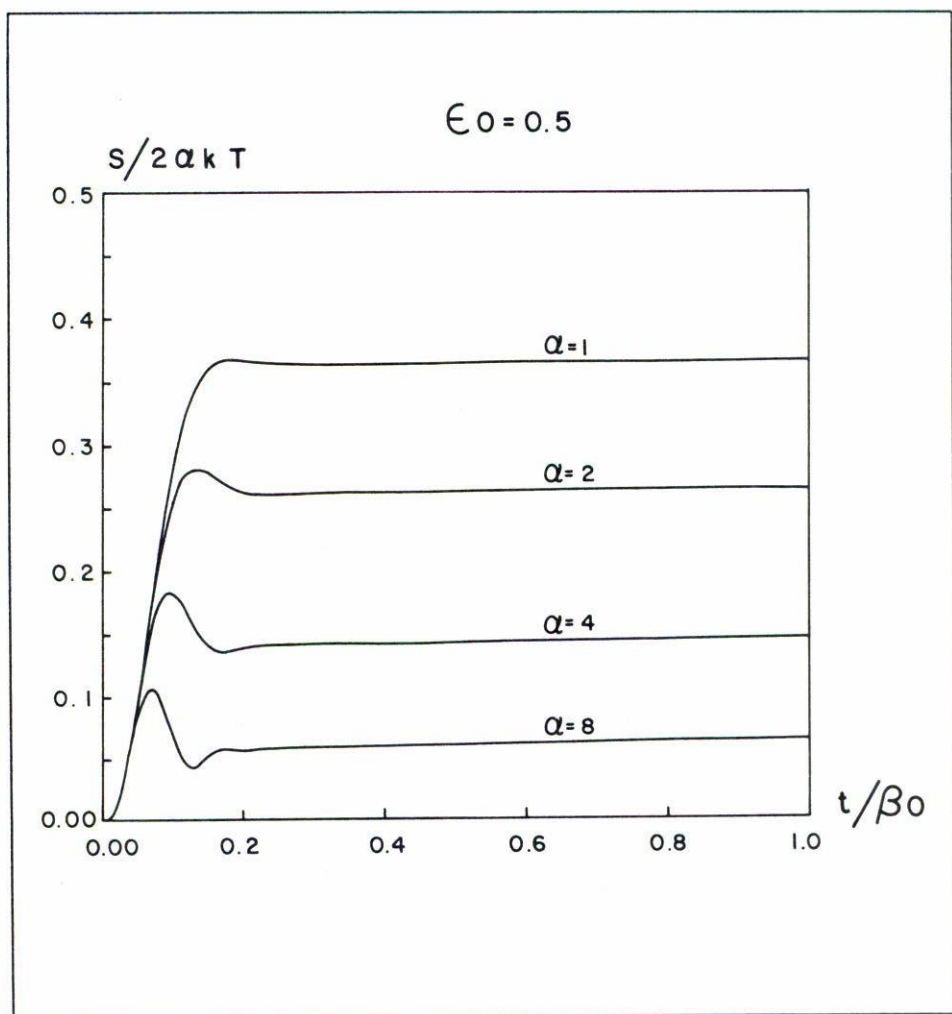


FIGURE 5. Same as in Fig. 3, with conformation-dependent slip parameter ($\epsilon_0 = 0.5$).

A conformational dependence of ϵ will allow for an independent variation of N_2 , as it is shown in Fig. 7.

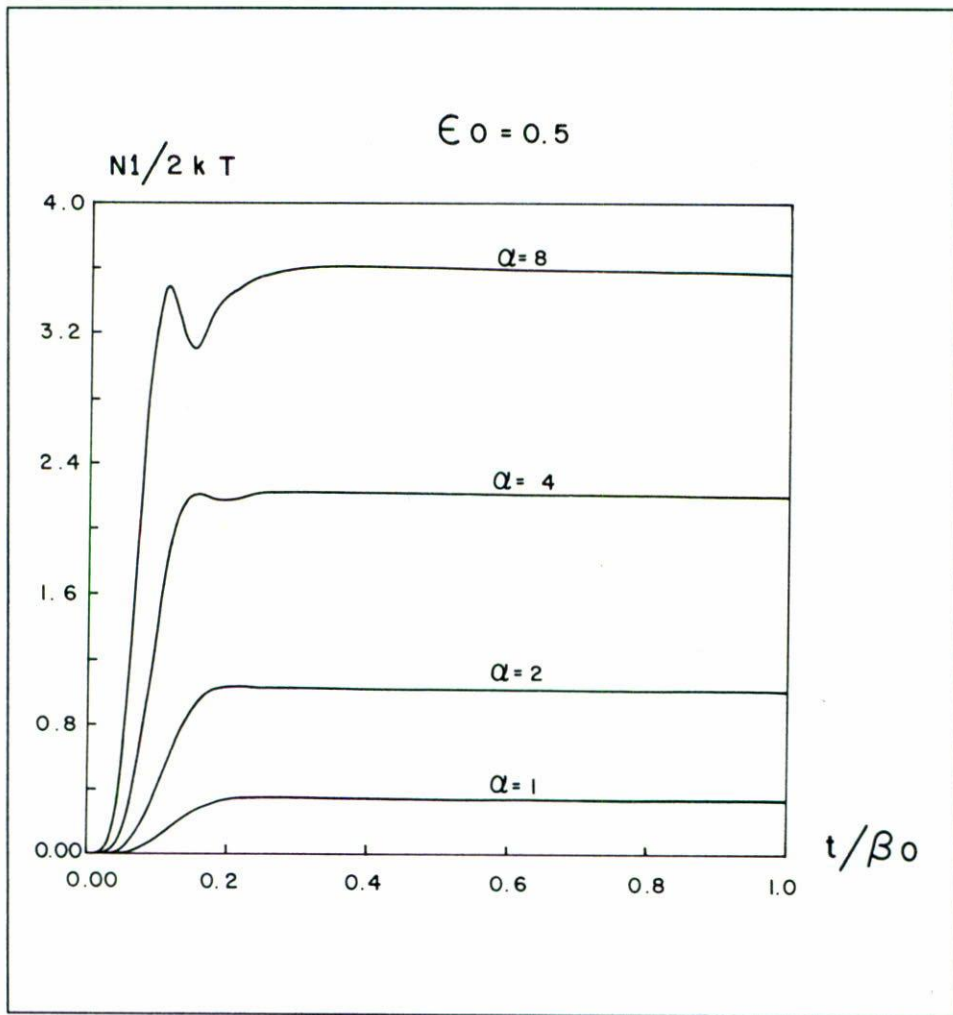


FIGURE 6. First normal-stress difference vs. non-dimensional time, for various values of the velocity gradient. Non-affine motion with conformation-dependent slip parameter ($\epsilon_0 = 0.5$).

8. Conclusions

In this work, attention was given to the rheological predictions

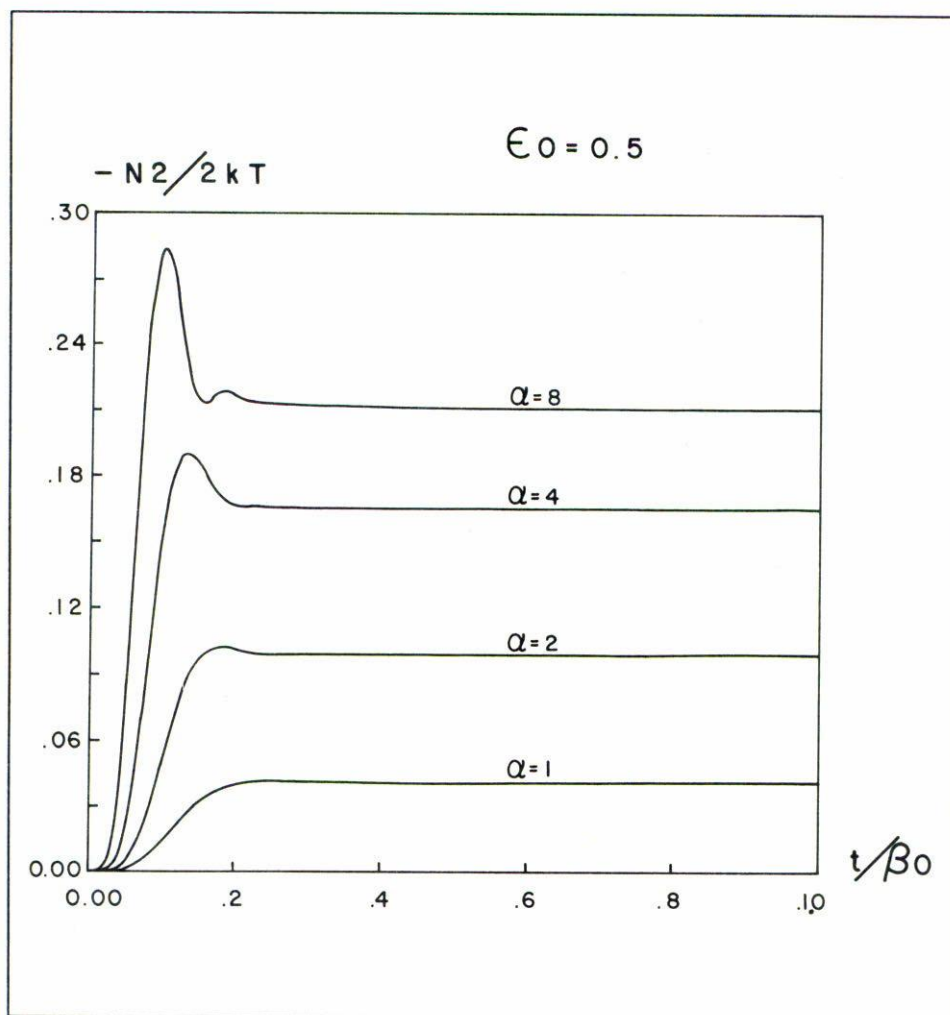


FIGURE 7. Second normal-stress difference vs. non-dimensional time. Same situation as in Fig. 6.

obtained from transient network models. The macroscopic effect of a conformation-dependent slip parameter corresponding to non-linear forces on the segments joining the network junctions is analyzed. In

addition, a conformation-dependent destruction function give rise to predictions of these models in the non-Gaussian regime of deformations. Results were presented in simple shear flow for both steady and unsteady state regimes that agree with experimental data exhibited by concentrated polymeric solutions in flow.

References

1. Green and Tobolsky, *J. Chem. Phys.* **14** (1946) 80.
2. A.S. Lodge, *Trans. Faraday Soc.* **52** (1956) 120.
3. M. Yamamoto, *J. Phys. Soc. Jpn.* **11** (1956) 413; **12** (1957) 1148; **13** (1958) 1200.
4. N. Phan-Thien and R. Tanner, *J. Non-Newt. Fluid Mech.* **2** (1977) 353.
5. M.W. Johnson and O. Segalman, *J. Non-Newt. Fluid Mech.* **2** (1977) 255.
6. R.B. Bird, R.C. Armstrong and O. Hassager, *Dynamics of Polymeric Liquids*, Vols. 1 and 2, Wiley, N.Y. (1977).
7. A. Peterlin, *Polymer* **2** (1961) 257.
8. Y. Rabin and J. W. Dash, *Macromolecules* **18** (1985) 442.
9. G.G. Fuller and L.G. Leal, *J. of Pol. Sci. Pol. Phys.* **19** (1981) 531.
10. N. Murayama, *Col. and Pol. Sci.* **259** (1981) 724.
11. A. Peterlin, *Pure and Appl. Chem.* **12** (1966) 563.
12. N. Phan-Thien, O. Manero and L. G. Leal, *Rheolg. Acta* **23** (1984) 151.